Cell Prolif. 1994, **27**, 73–94

Analysis of growth of multicellular tumour spheroids by mathematical models

M. Marušić*§, Ž. Bajzer†, J. P. Freyer‡ and S. Vuk-Pavlović*†

**Division of Developmental Oncology Research and †Department of Biochemistry and Molecular Biology, Mayo Clinic and Mayo Foundation, Rochester, MN and ‡Life Sciences Division, Los Alamos National Laboratory, Los Alamos, NM, USA*

§On leave of absence from the Department of Mathematics, University of Zagreb, Zagreb, Croatia

(*Received* 11 *March* 1993; *revision accepted* 6 *May* 1993)

Abstract. We wished to determine the applicability of previously proposed deterministic mathematical models to description of growth of multicellular tumour spheroids. The models were placed into three general classes: empirical, functional and structural. From these classes, 17 models were applied systematically to growth curves of multicellular tumour spheroids used as paradigms of prevascular and microregional tumour growth. The spheroid growth curves were determined with uniquely high density of measurements and high precision. The theoretical growth curves obtained from the models were fitted by the weighted least-squares method to the 15 measured growth curves, each corresponding to a different cell line. The classical growth models such as von Bertalanffy, logistic and Gompertz were considered as nested within more general models. Our results demonstrate that most models fitted the data fairly well and that criteria other than statistical had to be used for final selection. The Gompertz, the autostimulation and the simple spheroid models were the most appropriate for spheroid growth in the empirical, functional and structural classes of models, respectively. We also showed that some models (e.g. logistic, von Bertalanffy) were clearly inadequate. Thus, contrary to the widely held belief, the sigmoid character of a three or more parameter growth function is not sufficient for adequate fits.

Interest in mathematical modelling in tumour biology results from the ability of models to describe and predict neoplastic growth. Consequently, numerous models have been proposed using both phenomenological and mechanistic descriptions of tumour growth. The plethora of mathematical approaches resulted in the need for comparative studies of the applicability of mathematical models to particular experimental systems, especially with regard to the notion that 'most contradictory theoretical models can be supported by the same observational material' (Feller 1971). However, few comparative studies are available (e.g. Vaidya & Alexandro 1982, Michelson, Glicksman & Leith 1987), partly because of the lack of suitable experimental data. Thus, we wish to examine systematically the applicability of mathematical models to carefully measured growth curves in well-understood experimental paradigms.

A particularly convenient experimental tumour paradigm is provided by the multicellular tumour spheroids culture system (Sutherland 1988, Bjerkvig 1992). Spheroids provide a system

Correspondence: Dr S. Vuk-Pavlović, Mayo Clinic, Rochester, MN 55905, USA.

for study of the prevascular phase of tumour growth in the absence of tumour–host interactions, and for investigating the regulation of growth by three-dimensional cell–cell interactions. Moreover, the growth curve for tumour spheroids can be conveniently determined with uniquely dense measurements and high precision (Freyer & Sutherland 1986b).

In this study we apply a large number (17) of classical and more recent deterministic mathematical models to spheroid growth curves derived from a large number (15) of tumour cell lines. In statistical discrimination among models we used the detailed analysis of residuals and, where applicable, the principle of nested models. In the forthcoming text, we analyse briefly the considered mathematical models for their formal relationships and present the experimental data, mathematical and statistical methods and the application to tumour spheroids.

MATHEMATICAL MODELS

A mathematical model of tumour growth is a mathematical expression of the dependence of tumour size on time. In the case of multicellular spheroids, growth follows the sigmoid curve with three distinct phases: the initial exponential phase, the linear phase and the plateau (Landry, Freyer & Sutherland 1982). For this study, we selected mathematical models that reflect the sigmoid nature of growth. The models include: **1** empirical models; **2** functional models (based on cell kinetics), and **3** structural models (developed specifically for spheroid growth).

Empirical models

These models are based on the fundamental empirical insight that growth results from the increase in size concomitant with processes that limit the size of the system. We considered two sets of empirical models developed for growth of biological systems.

One set of models is based on the principle that for tumour size V, the rate of change in size $V' \equiv dV/dt$ is a difference between the rate of growth and the rate of degradation. According to von Bertalanffy (1957), both rates follow the law of allometry, i.e. they are proportional to the power of tumour volume, so the growth equation is of the form:

$$V' = aV^{\alpha} - bV^{\beta},\ V(0) = V_0 \tag{1}$$

(Starting from different assumptions, Savageau (1979) later derived the same equation.) Recently we solved equation (1) and obtained an explicit expression for V (Marušić & Bajzer 1993). However, we found that it was more convenient to solve the differential equation (1) numerically than to evaluate our rather complex expression that involves functions not included in standard mathematical program libraries.

As special cases, equation (1) includes the well known logistic growth equation (Verhulst 1838, Pearl 1924):

$$V' = aV - bV^2,\ V(0) = V_0, \tag{2}$$

with the solution

$$V = \frac{a}{b}\left[1 - \left(1 - \frac{a}{bV_0}\right)e^{-at}\right]^{-1}, \tag{3}$$

and the von Bertalanffy (1941) growth equation:

$$V' = aV^{\frac{2}{3}} - bV,\ V(0) = V_0, \tag{4}$$

with the solution

$$V = \left[\frac{a}{b} + \left(V_0^{\frac{1}{3}} - \frac{a}{b}\right)e^{-bt/3}\right]^3. \tag{5}$$

Both models have been used for description of tumour growth (Vaidya & Alexandro 1982).

It is interesting that a particular limiting case of equation (1) is the most often used Gompertz equation (Gompertz 1825):

$$V' = aV - bV \ln V,\ V(0) = V_0, \tag{6}$$

with the solution

$$V = e^{\frac{a}{b} - (\frac{a}{b} - \ln V_0)e^{-bt}}. \tag{7}$$

When parameters α and β approach 1, the growth curve represented by equation (1) does not necessarily approach an exponential curve, but it may also approach the Gompertz growth curve. Indeed, when equation (1) is rewritten in terms of parameters $c = a - b$, $d = \varepsilon b$, $\varepsilon = \beta - \alpha$ as: $V' = cV^{\alpha} - dV^{\alpha}(V^{\varepsilon} - 1)/\varepsilon$, it appears that for $\varepsilon \to 0$ and $\alpha \to 1$ the form of equation (6) is obtained. Furthermore, we have shown (Marušić & Bajzer 1993), that the solution of rewritten equation (1) approaches the solution of equation $V' = cV - dV \ln V$ as $\varepsilon \to 0$, $\alpha \to 1$ and that equation (1) contains the more general equation

$$V' = aV^{\alpha} - bV^{\alpha} \ln V,\ V(0) = V_0, \tag{8}$$

as a special case. We designated this equation the 'generalized Gompertz equation' (Marušić & Bajzer 1993). As for equation (1), the solution of equation (8) can be conveniently obtained by solving it numerically rather than by evaluating the corresponding expression (Marušić & Bajzer 1993).

Finally, equation (1) contains also a special case of the form

$$V' = \begin{cases} aV^{\alpha} - bV, & \alpha < 1, \\ \alpha V - bV \ln V, & \alpha = 1, \\ \alpha V - bV^{\alpha}, & \alpha > 1, \end{cases} \quad V(0) = V_0, \tag{9}$$

with the solution

$$V = \begin{cases} [\frac{a}{b} - (\frac{a}{b} - V_0^{1-\alpha})\, e^{-b(1-\alpha)t}]^{1/(1-\alpha)}, & \alpha < 1, \\ e^{\frac{a}{b} - (\frac{a}{b} - \ln V_0)e^{-bt}}, & \alpha = 1, \\ [\frac{b}{a} - (\frac{b}{a} - V_0^{1-\alpha})\, e^{-a(\alpha-1)t}]^{1/(1-\alpha)}, & \alpha < 1, \end{cases} \tag{10}$$

which we designate the 'generalized Bertalanffy-logistic equation'.

Models given by equations (2), (4), (6), (8) and (9) are special cases of the model described by equation (1) and are nested (Bishop, Fienberg & Holland 1975) within this model. Figure 1 illustrates the nesting relationships. These relationships make it possible to compare the models by well-defined statistical criteria.

Another set of nested empirical models was proposed by Turner *et al.* (1976). They assumed that the rate of change in size is proportional to the product of one function increasing with size and the other function decreasing with size. The corresponding equation reads

$$V' = \frac{\beta}{k^n} V^{1-np} (k^n - V^n)^{1+p},\ V(0) = V_0, \tag{11}$$

where

$$-1 < p < \frac{1}{n},\ n > 0, \tag{12}$$

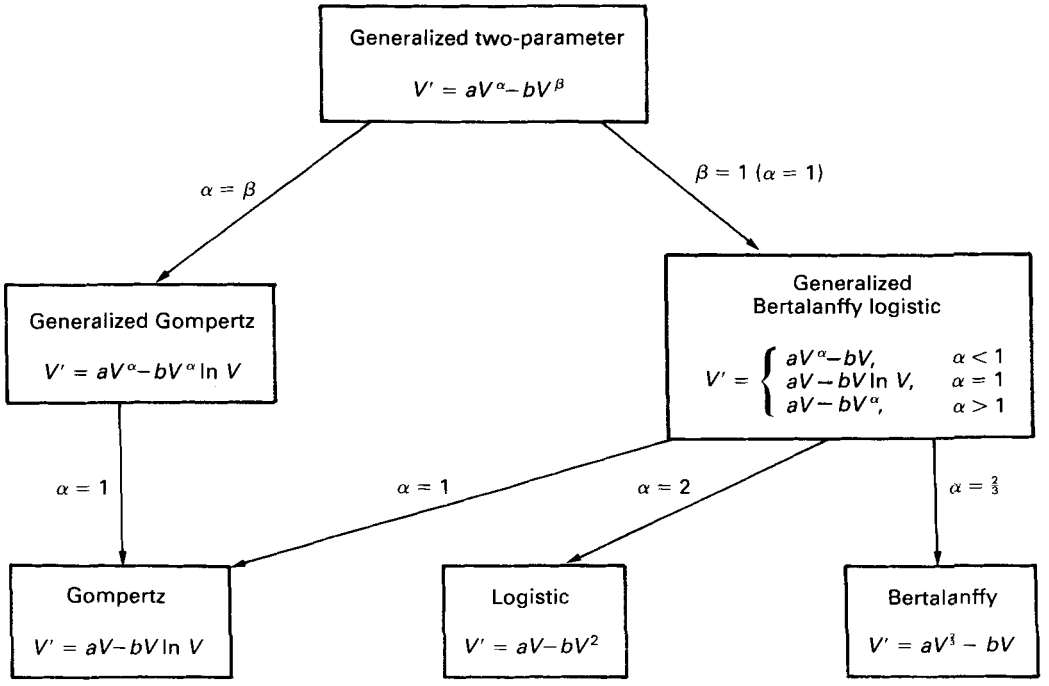

Figure 1. Nesting scheme for models originating from the generalized two-parameter model of growth.

and the solution designated as the 'generic growth curve' is

$$V = k\left\{1 + \left[\beta pnt + \left(\left(\frac{k}{V_0}\right)^n - 1\right)^{-p}\right]^{-1/p}\right\}^{-1/n} \tag{13}$$

Turner *et al.* (1976) derived the special cases of equation (11). One is the 'hyper-Gompertz' model:

$$V' = \beta V\left(\ln\frac{k}{V}\right)^{1+p}, V(0) = V_0, \tag{14}$$

with the solution

$$V = ke^{-[\beta pt + (\ln(k/V_0))^{-p}]^{-1/p}} \tag{15}$$

and the other is the 'hyper-logistic' model

$$V' = \frac{\beta}{k} V^{1-p}(k - V)^{1+p}, V(0) = V_0, \tag{16}$$

with the solution

$$V = k\left\{1 + \left[\beta pt + \left(\frac{k}{V_0} - 1\right)^{-p}\right]^{-1/p}\right\}^{-1} \tag{17}$$

For $p = 0$ the generic equation reduces to the Bertalanffy–Richards equation (cf. Turner *et al.* 1976) which is a special case of the generalized Bertalanffy-logistic model (equation (9); $\alpha > 1$). The Gompertz model (6) and the logistic model (2) are nested in the hyper-Gompertz and the hyper-logistic models, respectively. The complete nesting scheme is given in Figure 2.

Another considered empirical model is the 'Gomp-ex' model (Wheldon 1988). It is a combination of the often used exponential model and the Gompertz model. The differential equation for this model is:

$$V' = \begin{cases} \alpha V, & V < V_c, \\ \alpha V - \beta \ln \dfrac{V}{V_c}, & V \geq V_c, \end{cases} \qquad V(0) = V_0. \tag{18}$$

The solution is partly the exponential and partly the Gompertz function:

$$V = \begin{cases} V_0 e^{\alpha t}, & V < V_c \\ V_c e^{\frac{\alpha}{\beta}(1 - e^{-\beta(t - t_c)})}, & V \geq V_c, \end{cases} \tag{19}$$

where

$$t_c = \frac{1}{\alpha} \ln \frac{V_c}{V_0}. \tag{20}$$

This model describes explicitly the initial exponential spheroid growth. For $V_c = V_0$, the Gomp-ex equation reduces to the simpler Gompertz equation.

Functional models

From the fertile field of functional models based on cell kinetics, we selected some with few parameters. Thus, we considered the model by Piantadosi (1985), the 'inhibition model'

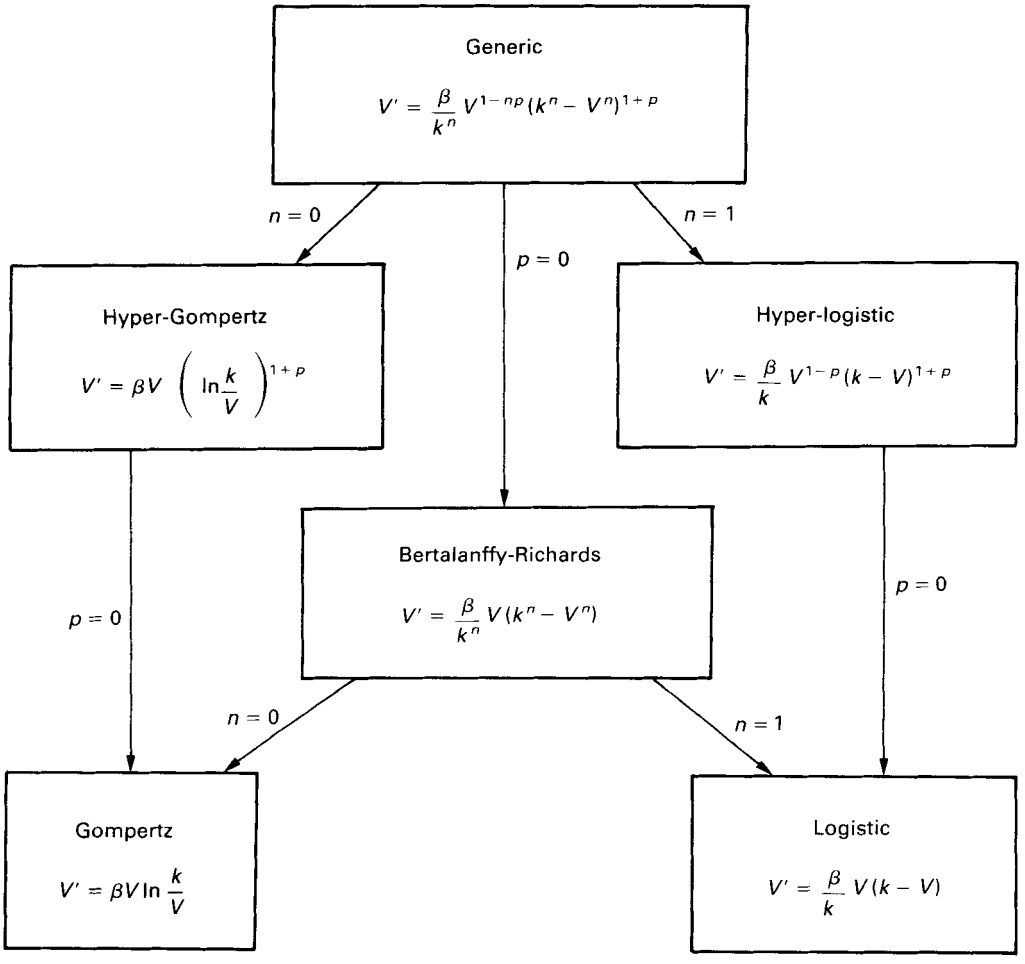

Figure 2. Nesting scheme for models originating from the generic model. Modified from Figure 1 in Turner *et al.* (1976).

formulated on the basis of work by Wheldon, Kirk & Gray (1973) and Cox, Woodbury & Myers (1980) as well as our 'autostimulation model' (Marušić *et al.* 1991) based on the autocrine hypothesis (cf. Bajzer & Vuk-Pavlović 1990). These models are characterized by the cellular doubling time, the fraction of actively dividing cells (growth fraction), and the random loss of cells from population. The magnitude of the growth fraction depends on the population size. The models and their nesting relationships are depicted in Figure 3. The solutions of the corresponding differential equations were obtained numerically.

We demonstrated (Bajzer, Marušić & Vuk-Pavlović 1993) that all three models can be derived from fundamental postulates of the cell cycle (Piantadosi 1985). The model by Wheldon *et al* (1973) and Cox *et al.* (1980) is a simple specialization of the model of Piantadosi (1985). The autostimulation model differs from the Piantadosi model in the expression for growth fraction; in both models these expressions are somewhat arbitrary.

The models in Fig. 3 account for volumes, though originally they were developed for cell numbers (Piantadosi 1985, Wheldon, Kirk & Grey 1973, Cox *et al.* 1980, Marušić *et al.* 1991). Although the total spheroid volume is not directly proportional to the number of living cells due to changes in cell size and central necrosis during growth (Freyer & Sutherland 1986a,b, Freyer 1988), these changes do not alter the overall size of the spheroid. Consequently, the spheroid volume can be substituted for the cell number in these models. This substitution makes it possible to apply the functional models to the measurements of spheroid volumes discussed in this paper.

Structural models

Several mathematical models have been developed for description of spheroid growth in structural terms. All such models assume that the spheroid is a perfect sphere and that processes such as proliferation, necrosis, diffusion, shedding, inhibition, etc., obey spherical symmetry. Thus the growth of a spheroid can be conveniently described by its radius, $R(t)$. However, the corresponding equations can be obtained in terms of volume by substitutions $V = 4/3\pi R^3$ and $V' = 4\pi R^2 R'$.

Conger & Ziskin (1983) based their 'constant crust' model on the observation that cells proliferate at a constant rate α within the proliferating cell rim of the spheroid; the rim is of

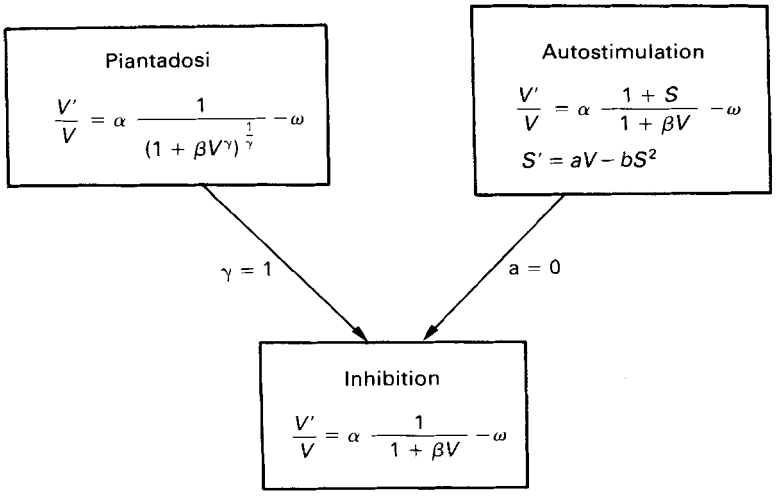

Figure 3. Nesting scheme for functional models. Initial conditions were $V(0) = V_0$; for the autostimulation model, they were $V(0) = V_0$ and $S(0) = 0$.

constant thickness, k (Landry, Freyer & Sutherland 1982). This model was modified by Wheldon (1988)*:

$$R' = \begin{cases} \frac{1}{3}\alpha R, & R \le k, \\ \alpha R\left[\frac{k}{R} - \left(\frac{k}{R}\right)^2 + \frac{1}{3}\left(\frac{k}{R}\right)^3\right], & R > k, \end{cases} \qquad R(0) = R_0. \tag{21}$$

The model describes the exponential and the linear phases of spheroid growth. The solution of equation (21) is unbounded. Consequently, it does not describe the final plateau phase.

To include the loss of cells, we modified equation (21) in analogy to the previous models:

$$R' = \begin{cases} \left(\frac{1}{3}\alpha - \omega\right)R, & R \le k, \\ \alpha R\left[\frac{k}{R} - \left(\frac{k}{R}\right)^2 + \frac{1}{3}\left(\frac{k}{R}\right)^3\right] - \omega R, & R > k, \end{cases} \qquad R(0) = R_0. \tag{22}$$

Again, the loss is assumed to be proportional to spheroid volume, with the rate of loss characterized by the rate constant 3ω. Due to simplicity of assumptions, we named this model the 'simple spheroid model'.

A more complex model was developed for growth of tumour spheroids by Landry *et al.* (1982). It is based on the following fundamental assumptions.

i. The proliferation rate of cells in the viable rim is proportional to the number of cells with the rate constant α.

ii. Proliferation occurs only if concentration of endogenous growth inhibitory factors is below a certain critical concentration. Concentrations of these factors behave according to the diffusion equation with the rate of diffusion δ, the decay rate $K^2\delta$ and the permeability K/η.

iii. The loss of cells from the viable rim is caused by necrosis of cells on the inner side of the rim and by shedding of cells from the outer side of the rim. Shedding is proportional to the surface of the spheroid and starts when $R = R_s$.

iv. The thickness k of the viable rim is constant for $R < \bar{R}$ ($\bar{R}$ is the radius at which the critical concentration of inhibitory factors is achieved in the viable rim).

Here we rewrite the model by Landry *et al.* (1982) in a more compact form:

$$R' = \frac{\alpha R_c G_1 - \beta F}{G_2 + (1 - H)G}, \tag{23}$$

where

$$R_c = \begin{cases} k, & R \le \bar{R}, \\ R - r(R), & R > \bar{R}, \end{cases} \tag{24}$$

$$G_1 = R - RR_c + R_c^2/3,\ G_2 = 2R - RR_c + R_c^2, \tag{25}$$

$$G = (R - R_c)^2,\ F = R^2 - R_s^2, \tag{26}$$

$$H = \begin{cases} 1, R \le \bar{R}, \\ h, R > \bar{R}, \end{cases} \quad h = \frac{1}{g(Kr)}\left[g(KR) + \eta\frac{1 - f^{-2}(KR)}{(KR)^2[1 + \eta g(KR)]}\right], \tag{27}$$

$$f(x) = \frac{\sinh x}{x},\ g(x) = \coth x - \frac{1}{x}. \tag{28}$$

*Note the errors in equations (5.46) and (5.47) in Wheldon (1988), corresponding to our equation 21.

The function $r(R)$ is given implicitly by

$$f(Kr) = af(KR)(1 + \eta g(K\bar{R})), \tag{29}$$

where a is determined by the requirement for continuity of R_c at $\bar{R}$; $\bar{R} - r(\bar{R}) = k$:

$$a = \frac{f(K(\bar{R}-k))}{f(K\bar{R})} \cdot \frac{1}{1+\eta g(K\bar{R})}. \tag{30}$$

Altogether there are eight adjustable parameters of the model: α, β, $\bar{R}$, k, R_s, η, K and R_0. It is interesting to note that the derivative R' in this model is discontinuous at $R = \bar{R}$ (because $H(\bar{R}+) > 1 = H(\bar{R}-)$).

Models not included

In the present study, we did not include all known mathematical models applicable to spheroid growth. For example, we did not include the models by Maggelakis & Adam (1990) and by Casciari, Sotirchos & Sutherland (1992) for complexity and computational requirements. For the same reason we did not consider the family of growth models proposed by Piantadosi (1987).

DATA

For this study we used the previously published data (Freyer 1988). The characteristics of individual data sets are summarized in Table 1. It is noteworthy that the spheroids were cultured under very uniform external conditions for the data used herein, both when comparing different data sets as well as during the course of any individual growth period.

In the forthcoming text, the data are presented as 'measurements'. A measurement refers to the mean volume V_i of 50 individual spheroids at any given time t_i ($i = 1, \ldots, n$). For each data set we calculated the relative standard errors, $r_i = \sigma_i / V_i$ and found that the average of r_i was approximately 0.02 (Table 1) with the standard deviation approximating 0.001. Thus, the standard error of the measurement σ_i was approximately proportional to the volume V_i for all data sets.

Table 1. Assignation of data, number of measurements (the mean volume of 50 individual spheroids at any given time) and error in measurement (for experimental details see Freyer (1988))

Data set no.	Cell line	Cell type	No. of measurements	Duration of expt/day	MRSE
1	MAC2	Adenocarcinoma	25	42.51	0.017
2	MCC26	Colon carcinoma	24	29.11	0.021
3	EMT6/Ro	Mammary carcinoma	33	49.17	0.018
4	MLC2	Lung carcinoma	27	37.56	0.022
5	PIN	Fibrosarcoma	39	49.15	0.018
6	V79	Fibroblast	45	59.38	0.015
7	CHO-K1	Fibroblast	28	40.12	0.017
8	CHO-XRS	Fibroblast	28	40.12	0.018
9	CHL-O23	Fibroblast	28	40.18	0.014
10	9L	Gliosarcoma	48	70.17	0.018
11	RF1	Fibrosarcoma	34	46.16	0.018
12	HCC1	Colon carcinoma	23	28.57	0.020
13	HLC1	Lung carcinoma	30	39.62	0.015
14	HT1080	Fibrosarcoma	44	55.23	0.020
15	MEL28	Melanoma	44	55.46	0.016

MRSE, Mean relative standard error $= \frac{1}{n}\sum_{i=1}^{n} \sigma_i / V_i$.

STATISTICAL AND COMPUTATIONAL METHODS

The best-fit curve for the model applied to any data set was obtained by the weighted least squares method, i.e. by minimization of the function

$$\chi^2 = \sum_{i=1}^{n} \left(\frac{V_i - V(t_i)}{\sigma_i} \right)^2 \tag{31}$$

over model parameters. In equation (31), V_i stands for the measured volume at time t_i, $V(t_i)$ for the corresponding volume computed from the model and σ_i for the standard deviation of V_i. The least squares method can be meaningfully applied when errors in measurement are distributed normally. Measurements used in this paper were obtained as means of 50 volumes and, consequently, the error distribution can be expected to approach the normal distribution.

Some considered differential equations were solved analytically and some numerically by the use of computer code ODEN (Shampine & Gordon 1975) The non-linear equation (29) was solved numerically by the subroutine NS01 from the Harwell Subroutine Library. For nonlinear minimization of the χ^2 function (31), we combined the Nelder–Mead simplex (Press *et al.* 1986) and the Levenberg–Marquardt minimization procedures (More 1977). To satisfy the non-negativity constraints on parameters mandated by the models, we used the penalty functions.

The quality of the fits was analysed by testing the normality of residuals

$$r_i = \frac{V_i - V(t_i)}{\sigma_i} \tag{32}$$

using the χ^2 goodness-of-fit test and the Kolmogorov–Smirnov goodness-of-fit test (Kreyszig 1970). Further, we tested the serial correlation of residuals r_i by use of the Durbin–Watson test (Durbin & Watson 1950, 1951).

The nesting of some models (Figures 1–3) allowed the selection of the most applicable model(s) by the *F*-test (see e.g. Cook & Weisberg 1990). The *F*-test is based on the statistic

$$f = \frac{(n - m_2)[\chi^2(m_1) - \chi^2(m_2)]}{(m_2 - m_1)\chi^2(m_2)}, \tag{33}$$

which follows approximately the *F*-distribution with $m_2 - m_1$ and $n - m_2$ degrees of freedom. Here the values of $\chi^2(m_1)$ and $\chi^2(m_2)$ correspond to the least χ^2 values obtained for the nested models defined by m_1 and m_2 free parameters, respectively ($m_2 > m_1$).

The fits by models not related by nesting can be compared by the Bayes information criterion (BIC) according to Schwarz (1978):

$$\mathrm{BIC} = \chi^2(m) + \frac{m}{2} \ln n. \tag{34}$$

where m is the number of free parameters and $\chi^2(m)$ corresponds to the least χ^2 value. The test is applicable when $\chi^2(m)$ is distributed by χ^2-distribution with the expected value $n - m$. Sometimes the value of $\chi^2(m)$ is larger due to underestimated measurement errors σ_i estimated by, say $\bar{\sigma}_i$. Then, the standard deviation can be estimated from the fit to a flexible function which is likely to yield low χ^2 value (say $\chi^2_1(m_1)$) and the fit is characterized by m_1 free parameters and by the normally distributed residuals. Namely, we can assume that standard deviations are given by $\sigma_i = \rho\bar{\sigma}_i$ and determine the factor ρ by imposing $\chi^2_1(m_1) = n - m_1$. This procedure implies that BIC takes the form used in this paper:

$$\mathrm{BIC} = (n - m_1)\frac{\chi^2(m)}{\chi^2_1(m_1)} + \frac{m}{2} \ln n. \tag{35}$$

The value of $\chi^2_1(m_1)$ was obtained by fitting polynomials to data. The polynomial function was

chosen because it is likely to provide a good description of data by an arbitrary number of parameters. We calculated the χ^2 values for polynomials of increasing order and chose the lowest order for which changes in χ^2 were no longer significant ($P \leq 0.05$ by F-test). According to above criterion, the preferred fit is characterized by smaller BIC, defined by equation (35).

RESULTS

A typical spheroid growth curve is shown in Figure 4. The curve exemplifies the three phases of spheroid development: exponential growth, linear growth and plateau. First, we fitted polynomial functions to all data sets. The fits yielded the χ^2 values which were too large in comparison to the expected value of $n-m$. For example, for the exemplary data set no. 6 the fit yielded the χ^2 value of 1687, while the expected value was $n-m=39$. However, the residuals were distributed normally and were not correlated for any but one data set (no. 10). The fit to the data set no. 10 was adequate by visual inspection, but the residuals appeared to be paired. Namely, the pairs of adjacent residuals were generally of similar magnitude and same sign, resulting in significant serial correlation. However, when the even-numbered residuals or the odd-numbered residuals were tested separately, there was no correlation. Therefore, in this case the observed serial correlation resulted probably from the error in data sampling rather than from their inadequate description. These findings imply the high likelihood that the polynomial model did provide an adequate description of the data and that the large χ^2 values resulted from the underestimated standard deviations in measurements of spheroid volume (cf. Press *et al.* 1986, p. 502). This conclusion is corroborated by the fact that the fits of other considered models to all data sets yielded large χ^2 values too (Table 2) and that for each but one data set (no. 10), there was at least one model with uncorrelated and normally distributed residuals (Table 3).

The exemplary best-fit curve in Figure 4 was obtained for the Gompertz model. The fit yielded the χ^2 value of 1797 (the expected value was 42). However, the residuals (Figure 4) were distributed normally and were not correlated.

Comparison of growth models by goodness of fit

The χ^2 values in Table 2 show that the logistic and von Bertalanffy models yielded fits inferior to other models (by the F-test $P < 10^{-4}$ relative to other models in the nesting schemes in Figures 1 and 2). Similarly, the constant crust model compared poorly with other models. In comparison to the simple spheroid model it gave a significantly worse fit. Therefore, in the further text we will not refer to the logistic, von Bertalanffy and constant crust models. Furthermore, we will not discuss fits by the four-parameter Gomp-ex model which coincided with the fits by the three-parameter Gompertz model for all data sets (i.e. all fits yielded $V_c = V_0$; see equation (18)).

Empirical models

All empirical models described the data similarly well. For most data sets, the χ^2-values for fits by all models were similar. For fits by the hyper-logistic model, the residuals were not distributed normally in five data sets; for all other models, the deviations from the normal distribution was observed in the data set no. 7 only (Table 3). The residuals were not serially correlated in any fit (except for data set no. 10, as discussed above).

The models belonging to the same nesting scheme were compared further by the F-test. Otherwise, we used the BIC. The fits for the generalized two-parameter, generalized Gompertz, generalized logistic-Bertalanffy and Gompertz models were equally good, except for data sets 12 and 13, where the Gompertz model yielded significantly different fits than the generalized Gompertz ($P=0.06$) and the generalized logistic-Bertalanffy models ($P=0.06$). As among

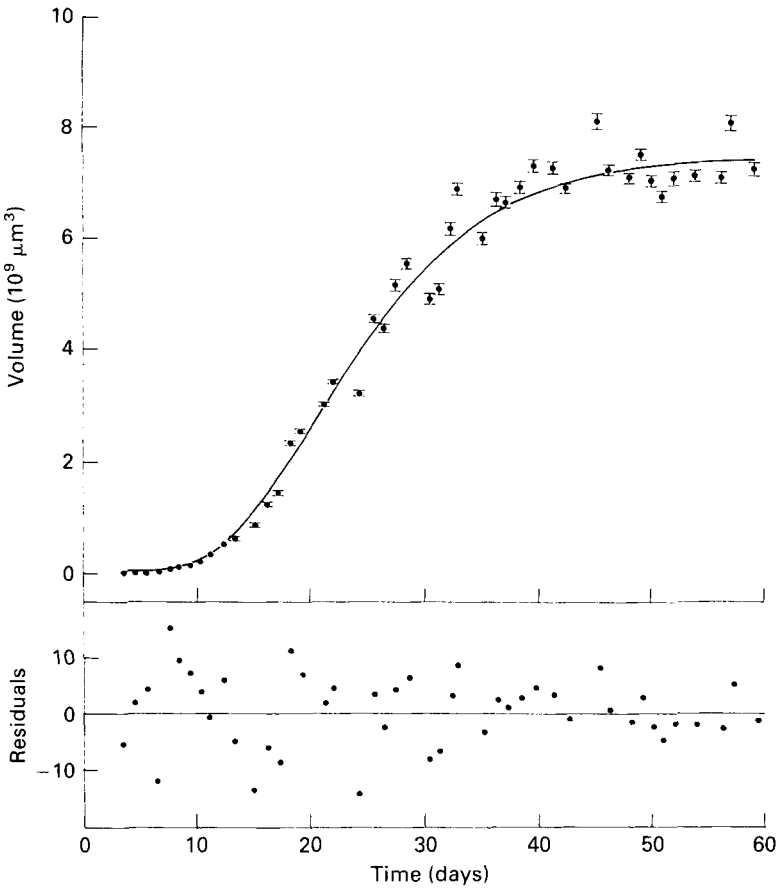

Figure 4. A typical spheroid growth curve (data set no. 6). The solid line was computed from the best fit parameters for the Gompertz model. The lower panel shows the residuals for the fit.

equivalent models the Gompertz model is characterized by the least number of parameters, it is the preferable description of the data. The exception to this rule (data sets 12 and 13) implicate the generalized logistic-Bertalanffy and generalized Gompertz models as more general descriptions that encompass all data sets.

The comparison of the generalized logistic-Bertalanffy model and the generalized Gompertz model by BIC (in this case, the comparison of χ^2 values) showed that the generalized Gompertz model fitted better in nine data sets. In other words, these models yielded quite comparable fits to spheroid growth curves. The proximity of the χ^2 minimum points in the (α, β) plane for fits by these models is illustrated in Figure 5 where the Gompertz, generalized Gompertz and generalized logistic-Bertalanffy models are shown as special cases of the generalized two-parameter model.

Comparison by the *F*-test showed that the Gompertz, hyper-Gompertz and Bertalanffy–Richards models fitted data equally well as the generic model. However, in ten data sets the hyper-logistic model resulted in significantly worse fits. As before, only for data sets 12 and 13 the fits by the Gompertz model were not equally good as the fits by the Bertalanffy–Richards and hyper-Gompertz models. This comparison indicated that the Gompertz model was the most applicable among those nested within the generic model (Figure 2). The BIC analysis of the

Table 2. The χ^2 values for empirical models, functional models and structural models. The values in the table were obtained by dividing the χ^2-value for the fit by each model by the χ^2 value for the respective fit by polynomials. The values for fits by polynomials are shown in the column designated Pol. together with the number of free parameters in parentheses

Data No. of free parameters	G* 3	GG 4	L 3	B 3	GBL† 4	GTP 5	HG 4	HL 4	Ge 5	AS 6	P 5	I 4	SS 4	LFS 8	Pol.	
1	1.448	1.391	88.838	50.880	1.391	1.391	1.409	2.324	1.376	1.183	1.338	5.372	2.059	2.084	55.2	(7)
2	0.875	0.876	22.005	13.218	0.876	0.876	0.876	1.316	0.873	0.912	0.872	2.903	1.331	0.884	318.3	(6)
3	1.048	1.045	8.045	5.903	1.045	1.045	1.047	1.303	1.030	0.873	1.007	1.418	1.037	1.028	1803.4	(7)
4	1.150	1.049	18.221	10.185	1.048	0.967	1.095	1.048	1.048	0.982	1.050	3.624	1.863	0.978	465.9	(5)
5	1.081	1.002	4.302	4.033	1.003	1.002	1.046	1.162	0.969	0.904	0.945	1.038	0.976	0.806	1856.0	(6)
6	1.038	0.987	12.653	7.568	0.987	0.972	1.011	1.069	1.011	0.882	0.987	2.654	1.410	0.968	1731.1	(7)
7	1.379	1.261	2.664	2.977	1.265	1.261	1.313	1.375	1.252	0.978	1.162	1.162	1.109	1.200	1559.2	(6)
8	1.067	1.039	18.806	9.757	1.039	1.039	1.054	1.141	0.972	0.813	1.022	1.574	1.226	0.752	168.9	(7)
9	1.287	1.175	26.653	10.663	1.175	1.174	1.185	1.371	1.185	1.284	1.176	2.780	1.553	1.287	446.8	(6)
10	1.033	1.031	10.303	7.079	1.031	1.031	1.030	1.214	1.030	1.043	1.031	1.658	1.288	1.179	2359.4	(7)
11	1.212	1.158	6.031	5.323	1.159	1.158	1.192	1.335	1.111	0.992	1.032	1.067	1.023	1.163	1291.6	(7)
12	1.414	1.158	16.098	12.016	1.158	1.158	1.122	1.334	1.122	0.971	1.158	1.861	1.342	1.437	145.4	(6)
13	1.157	1.011	4.701	4.780	1.011	1.011	1.039	0.996	0.996	1.011	1.011	1.178	1.098	0.928	731.8	(8)
14	1.124	1.113	10.658	8.889	1.113	1.113	1.115	1.403	1.113	0.968	1.107	2.234	1.324	1.067	1168.5	(8)
15	1.056	1.045	15.630	12.645	1.045	1.044	1.041	1.257	1.041	1.088	1.045	2.591	1.531	1.262	1087.2	(9)

* χ^2 values for the Gomp-ex model (4 parameters) were identical to the Gompertz model.

† χ^2 values for the Bertalanffy–Richardson model (4 parameters) were identical as for the generalized Bertalanffy-logistic model, except for the data sets 2, 4, 6 and 9, where they were equal to the values computed for the Gompertz model.

G, Gompertz; GG, generalized Gompertz; L, logistic; B, Bertalanffy; GBL, generalized Bertalanffy-logistic; GTP, generalized two-parameter; HG, hyper-Gompertz; HL, hyper-logistic; Ge, generic; AS, autostimulation; P, Piantadosi; I, inhibition; SS, simple spheroid; LFS, Landry *et al.* (1982); Pol., polynomial.

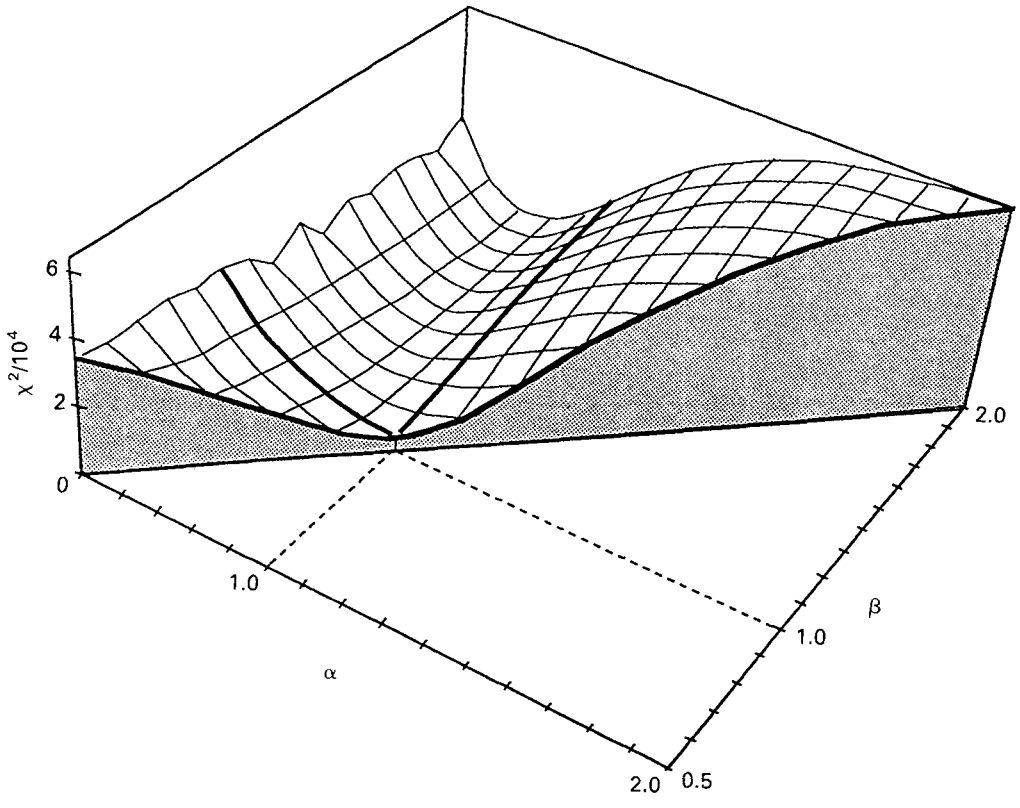

Figure 5. The dependence of χ^2 values on parameters α and β in the generalized two-parameter model for the data set no. 8. Each point in the grid was calculated for the fixed values of α and β by minimization over the remaining parameters. The domain $\alpha = \beta$ indicates the χ^2 values for the generalized Gompertz model; the domain $\alpha = 1$ or $\beta = 1$ stands for the generalized logistic-Bertalanffy model. The point $\alpha = \beta = 1$ indicates the χ^2 value for the Gompertz model.

four-parameter generalized logistic-Bertalanffy and hyper-Gompertz models demonstrated the preference for the generalized logistic-Bertalanffy model (11 data sets with smaller χ^2). Also, the generalized Gompertz model was preferable to the hyper-Gompertz model in 11 data sets. In conclusion, this analysis of empirical models showed that the Gompertz model was preferable for description of spheroid growth curves.

Functional models

Fits by the functional models based on cell kinetics (Figure 3) are presented in Table 2. The comparison of fits by the inhibition model and the autostimulation model (F-test) showed that the difference in χ^2 values was significant in 11 data sets. This difference was significant also for fits to 13 data sets by the inhibition model and the Piantadosi model. Importantly, the residuals in eight fits by the inhibition model were significantly serially correlated (Table 3). Thus, the inhibition model appeared inadequate for description of these data. The comparison of fits by the autostimulation model and the Piantadosi model by BIC did not show marked preference. For the former model, BIC was larger for eight data sets whereas the BIC calculated for the Piantadosi model was larger for seven data sets.

Table 3. Statistical analysis of residuals obtained in fits to spheroid growth data

Data		G	GG	GBL	GTP	HG	HL	Ge	AS	P	I	SS	LFS
1	N*										0.025	IC	IC
2	N						0.08						
	C										IC		
3	N						0.07						0.01
	C	IC	IC	IC	IC	IC	0.05	IC	IC	IC	0.025	IC	IC
4	N												
	C	IC	IC	IC		IC		IC		IC	0.025	IC	IC
5	N						0.04			0.06			
	C												
6	N					0.098							
	C												
7	N	0.02	0.003	0.003	0.003	0.002	0.03	0.02		0.03	0.03	0.05	0.08
	C												
8	N						0.09						
	C		IC	IC	IC	IC	IC			IC	IC		
9	N												
	C		IC	IC	IC	IC	IC	IC		IC	0.05	IC	IC
10	N												
	C	0.025	0.025	0.025	0.025	0.025	0.025	0.025	0.025	0.025	0.025	0.025	0.025
11	N										0.06		
	C		IC	IC	IC	IC	IC	IC					IC
12	N											0.095	
	C				IC			IC		IC	IC	IC	IC
13	N												
	C												
14	N										0.02		
	C										0.025	IC	
15	N												0.06
	C										0.025	IC	IC

IC, inconclusive: the test cannot discriminate between the options.

Abbreviations as for Table 2.

*For each data set/model combination the upper lines (N) show the significance that he residuals are not distributed normally. The lower lines (C) show the significance that the residuals are serially correlated. Blanks indicate the absence of significance at the level of 0.1.

The goodness-of-fit tests revealed that the distribution of residuals in all fits by the autostimulation model did not deviate from the normal, while in fits by the Piantadosi model they did deviate for three data sets. Also, for the autostimulation model the residuals were not significantly serially correlated in more data sets than for the Piantadosi model (Table 3). Thus, by the analysis of residuals, the autostimulation model appears applicable to a larger number of data sets.

Structural models

The χ^2 values for the simple spheroid model were commensurate with the respective values for other models that yielded acceptable fits (Table 2). For three data sets this model resulted in notably larger χ^2 values, but the residuals for these fits were still distributed normally and were not correlated. Also, in three data sets the distribution of residuals differed significantly from the normal. In a comparison of the fits by the BIC, the simple spheroid model was preferred over the Gompertz model in three data sets.

The model of Landry *et al.* (1982) fitted the data with the χ^2 values commensurate with other

models; for three data sets these values were the lowest (Table 2). Comparison by the BIC showed that the Gompertz model was clearly preferred (14 data sets).

It should be noted that for the model of Landry *et al.* (1982) minimization did not proceed smoothly, was more time consuming than for any other model and required more different initial parameter guesses. Despite every attempt to reach the minima, for this model we are less convinced that we indeed obtained the true global minima.

Comparison of cellular doubling times and viable rim thicknesses

Data available for cellular doubling times in two-dimensional cell culture and the viable rim thickness (Freyer 1988) provide limiting values with which to scrutinize the biological relevance of various models. Therefore, we compared the values estimated from the best fits of models found applicable for description of spheroid growth (Gompertz, autostimulation, Piantadosi, simple spheroid, Landry *et al.* (1982)) to these data.

Cellular doubling time

All functional and structural models include the proliferation rate as a model parameter. Therefore, it is possible to calculate the cellular doubling time, T_d, from best-fit parameters according to expressions:

$$\frac{\ln 2}{T_d} = \alpha, \tag{36}$$

for the autostimulation model, the simple spheroid model and the model by Landry *et al.* (1982) For the Piantadosi model two expressions are possible (cf. Figure 3):

$$\frac{\ln 2}{T_d} = \frac{\alpha}{(1+\beta V_0^{\gamma})^{1/\gamma}} \tag{37}$$

and

$$\frac{\ln 2}{T_d} = \frac{\alpha}{(1+\beta V_0^{\gamma})^{1/\gamma}} - \omega, \tag{38}$$

depending on the assumptions (Piantadosi 1985) that cells die in the entire population, equation (37), or just among quiescent cells (equation 38).

Also, the Gomp-ex model allows for calculation of the doubling time according to equation (36), as it describes the exponential phase of growth explicitly (cf. equation (18)). The Gomp-ex model yielded fits identical to the fits by the Gompertz model; consequently, the doubling time could be calculated from the best-fit parameters of the Gompertz model (cf. equations (6), (18)):

$$\frac{\ln 2}{T_d} = a - b \ln V_0. \tag{39}$$

The calculated T_d values are listed in Table 4 together with the doubling times measured for the corresponding cells in monolayer culture during exponential growth (Freyer 1988). All models resulted in estimated values of proper magnitude, except the model by Landry *et al.* (1982) with the calculated doubling times in excess of 1 year in four data sets. We found no correlation between experimental and calculated values for any model (linear regression and Spearman Rank correlation coefficient; for the model by Landry *et al.* (1982) the four outliers with $T_d > 1$ year were not taken into account).

To ascertain whether the meaning of T_d is consistent among structural and functional models, we correlated the computed T_d values for all possible model pairs and found that calculated doubling times for most model pairs were significantly correlated ($P < 0.05$). The exceptions were

model pairs Landry *et al.*/Piantadosi (for both possible T_d values in the latter model), Landry *et al.*/autostimulation, and Gompertz/Piantadosi (with T_d given by equation (37)).

Thickness of the rim of proliferating cells

The simple spheroid and the model by Landry *et al.* (1982) include parameter k which stands for the constant thickness of the rim of proliferating cells (cf. equations (22), (24)). The set of functional models does not assume the presence of the proliferating rim but the rim thickness can be deduced from the growth fraction f. For these models the proliferating rim thickness K is expressed as

$$K = \sqrt[3]{\frac{4}{3\pi}V}\left(1-\sqrt[3]{1-f}\right). \tag{40}$$

For the autostimulation model, the growth fraction is (cf. Figure 3):

$$f = \frac{1+S}{1+\beta V}, \tag{41}$$

while for Piantadosi model it is (cf. Figure 3):

$$f = \left(\frac{1+\beta V_0^{\gamma}}{1+\beta V^{\gamma}}\right)^{1/\gamma}. \tag{42}$$

In both models, the predicted thickness of the proliferating rim depended on volume (time), but varied within narrow limits after the maximum had been reached (Figure 6a). However, for some data sets the Piantadosi model resulted in much more prominent time dependence of the thickness than the autostimulation model (Figure 6b).

We used the measured thickness of the viable rim (Freyer 1988) for comparison with the thickness of the proliferating cell rim (k) calculated at the spheroid diameter of 1000 μm. The measured thickness of the viable rim refers to the morphologically intact cells measured in

Table 4. Experimentally determined cellular doubling times in culture and the computed doubling times in spheroids. The doubling times of cells in spheroids reported in Freyer (1988) were calculated from fits of the Gompertz model with fixed values of V_0

	Time (h)						
Data	Exp	G	AS	P_1	P_2	SS	LFS
1	12	11.3	15.8	11.7	19.6	14.9	> 1 year
2	13	8.7	13.1	9.3	14.4	14.5	13.1
3	9.5	13.7	17.1	18.8	22.4	20.6	14.6
4	17	7.6	12.2	4.4	13.1	13.8	4.2
5	20	11.6	19.9	21.0	26.1	18.9	7.6
6	10	10.7	14.3	4.4	15.4	15.2	2.3
7	13	10.7	36.3	23.5	28.6	15.2	13.2
8	14	14.3	11.5	16.1	25.8	17.8	5.3
9	15	13.5	18.7	6.9	20.2	18.7	> 1 year
10	18	20.3	19.4	9.6	27.7	29.2	12.2
11	12	9.2	17.4	19.2	22.3	15.0	7.4
12	18	8.9	8.9	4.0	17.3	12.1	> 1 year
13	15	6.1	6.7	2.4	17.4	10.8	> 1 year
14	11	13.3	18.8	12.4	20.6	19.6	6.9
15	10	9.4	14.6	2.8	16.0	15.1	1.8

Abbreviations as for Table 2.

Exp, experimental doubling times in cell culture; P_1, P_2, doubling times according to equation (37) and equation (38), respectively.

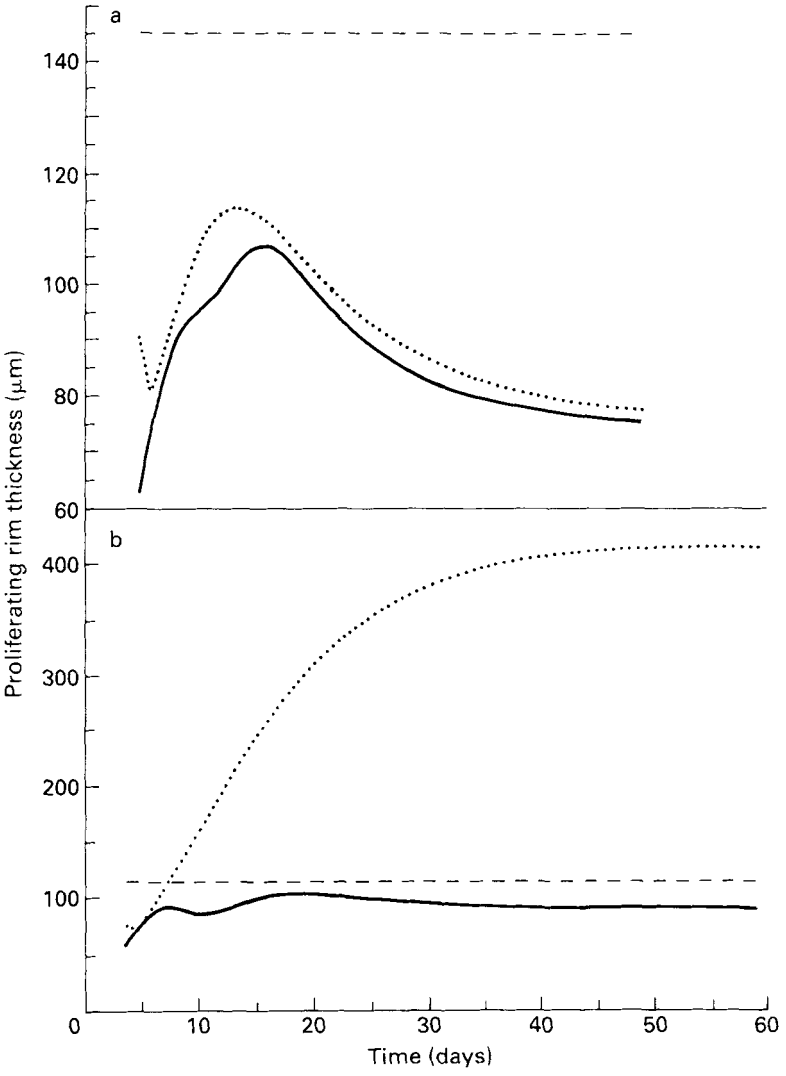

Figure 6. Proliferating rim thickness computed by the use of Piantadosi model and the autostimulation model. Computed for data sets **a** no. 5 and **b** no. 6, respectively. Solid line, autostimulation; dashed line, simple spheroid; dotted line, Piantadosi.

spheroid populations 800–1200 μm in diameter, without regard to the rate of division at different distances from the spheroid centre. Therefore, these values represent the upper possible limits for the calculated k, which stands for the thickness of the rim of cells dividing at a constant rate. For spheroids in this diameter range, the viable rim is actually composed of a mixture of cells proliferating at various rates, as well as cells which have completely ceased proliferation (Sutherland 1988, Freyer & Sutherland 1986a, Freyer & Schor 1989).

The model by Landry *et al.* (1982) did not result in calculated rim thickness within the range of the experimentally determined values. The simple spheroid model yielded the values of k on the average 25% smaller than measured viable cell rim. The autostimulation model predicted the

Table 5. Experimentally determined viable ring thickness and computed proliferating cell rim thickness (μm) in spheroids

Data	Exp	AS	P	P_l	SS	LFS
1	118	67	77	97	85	777
2	257	71	98	217	129	109
3	251	135	87	90	128	79
4	213	95	125	499	129	46
5	238	95	105	77	145	45
6	180	92	118	416	115	21
7	98	176	72	32	96	50
8	85	30	70	74	79	18
9	198	89	103	292	97	1007
10	225	47	123	515	157	69
11	139	99	86	39	107	39
12	176	89	116	196	84	739
13	104	31	138	239	97	571
14	228	108	91	210	129	48
15	135	109	152	500	124	17

Abbreviations as for Table 2.

P_l, rim thickness at the point of last measurement by the Piantadosi model. For AS and P models, the values are reported for spheroids of 1000 μm in diameters.

thickness of the proliferating cell rim on the average 55% smaller than the measured viable rim (Table 5, Figure 6). For the Piantadosi model, in seven data sets the predicted rim thickness exceeded the measured value (Table 5, Figure 6b).

The calculated values for k for the simple spheroid model were significantly correlated with the experimental values ($r^2 = 0.57$, $P = 0.0012$). For the model by Landry *et al.* (1982) such correlation was not found, but when the evident outliers (data sets 1, 9, 12 and 13) were left out, there was correlation ($r^2 = 0.44$, $P = 0.0264$). Note that the omitted data sets were those which yielded doubling times in excess of 1 year (Table 4). The values of the rim thickness predicted by the autostimulation model were not correlated with experimental values ($r^2 = 0.02$, $P = 0.628$). However, when the data set no. 7 was left out, correlation was marginal ($r^2 = 0.27$, $P = 0.058$). Data set no. 7 could be left out because the calculated growth fraction (equation (41)) exceeded the upper possible value of one (at the initial stage of growth) and the calculated doubling time for this data set was an evident outlier (Table 5). When the data set no. 10 (residuals serially correlated, Table 3) was omitted too, there was a significant correlation with experiment ($r^2 = 0.41$, $P = 0.018$). For the Piantadosi model the correlation between the calculated and experimental values was found neither for the spheroid diameter of 1000 μm nor at the end of experiment, even when the outliers were left out.

DISCUSSION

There has been a long-standing interest in testing mathematical models of growth on experimental tumours. The literature contains evidence of numerous models tested on a number of diverse experimental systems. In this work, we tested, systematically and comprehensively, several empirical, functional and structural models on measurements of growth of multicellular tumour spheroids. Spheroids were selected for their relative simplicity and for the large number of experimental data sets available under uniform conditions and at high data density. In addition,

the ability to precisely control the culture conditions in the spheroid system makes it possible to experimentally test predictions derived from mathematical modelling of growth.

The present study demonstrates that the choice of a particular model for description of spheroid or tumour growth data could not be decided from statistical analysis alone (Feller 1940, 1971, Press *et al.* 1986), but had to be based on the rationale behind the use of a specific model. However, our analysis could reject clearly inadequate models (von Bertalanffy, logistic, inhibition, constant crust). This finding demonstrates that the sigmoid character of a growth function is a necessary, but not sufficient condition for adequate fits; this contradicts the belief that any sigmoid function will yield a reasonably good fit, as implied by Gyllenberg & Webb (1989).

The Gompertz model is the empirical model of choice for studies in which precise description of the growth curve takes preference over understanding of mechanistic or biological aspects of growth, such as in optimization of therapy (Swan 1990). The functional models are applicable to studies directed toward the mechanistic understanding of the regulation of cell growth. In this class, the preference for the autostimulation model over models without the autostimulation terms is compatible with the role of positive feedback in cell–cell interactions. Finally, structural models stress geometric considerations in spheroid growth. The preference for the simple spheroid model over the model without cell loss indicates the quantitative role of cell loss in the growth of prevascular tumours. In the following discussion we will compare the goodness-of-fit for the various models in each class, and elaborate on the biological implications associated with the best model.

Amongst empirical models, it is intriguing that none of the six different generalizations was preferable to the original Gompertz model. This finding is in line with recent results by Michelson *et al.* (1987) and supports the notion by Steel that 'when the data cover a wide range of sizes the Gompertz equation usually gives the better fit than either the logistic or the Bertalanffy equation' (Steel 1977). As discussed by Swan (1990), the common view is that the Gompertz model is widely applicable. It is interesting that for spheroids the logistic and von Bertalanffy models are inadequate while for tumours *in vivo*, Vaidya & Alexandro (1982) found these models preferable to the Gompertz model. To ascertain whether the Gompertz model is preferable amongst the empirical models for a given data set, we recommend the application of the generalized Gompertz model or the generalized Bertalanffy-logistic model. The latter model is easier to implement for computation, but is numerically unstable when α approaches 1. The former model is less convenient for its requirement of numerical integration, but it appears to be more numerically stable.

Recently Gyllenberg & Webb (1989) analysed Gompertzian growth in terms of transition of proliferating cells into quiescence (absence of division) and *vice versa*. They showed that the Gompertzian growth was characterized by the rate of transition into quiescence which followed the logarithmic law; for the logistic growth this rate was characterized by the linear law. In spheroids, the Gompertz model clearly outperformed the logistic model indicating that the proliferating cells progressed into quiescence by a rate which followed the logarithmic law, rather than the linear law. It might be possible that the different best fit models for prevascular tumours (this work) and some vascularized tumours (Vaidya & Alexandro 1982) also result from different laws of transition of cells from proliferation to quiescence.

Comparisons of calculated doubling times *v.* measured monolayer doubling times were not conclusive. There was no correlation between the experimental and calculated values, and in most cases these doubling times agreed within a factor of two. Only the outermost cell layers in the spheroid enjoy the unrestricted access to the medium similar to cells in two-dimensional culture; consequently, only they will divide at a rate similar to the rate for cells in two-dimensional

exponentially growing culture. Cells closer to the spheroid center divide at a progressively slower rate (Freyer 1988). Therefore, it is expected that the division rates determined in cell culture represent the lower limits of the doubling times in spheroids (cf. Freyer 1988). In most cases, the doubling times predicted by the autostimulation model, the Piantadosi model and the simple spheroid model were larger than the experimental values. However, the predicted values and the experimental values were not correlated, precluding the use of these experimental data for definite selection of the most adequate model.

Amongst functional models, the inhibition model was relatively inadequate for description of spheroid growth. The generalizations of this model, such as the Piantadosi model and the autostimulation model, yielded adequate fits, but the thickness of the proliferating rim was predicted differently by the two models. The correlation between the predicted and the experimental values of the rim thickness was found for the autostimulation model only. This finding and the slightly better fits (in terms of normality of residuals and serial correlation) made the autostimulation model preferable among the functional models. Interestingly, this model predicted that the thickness of the proliferating cell rim was, on average, 55% of the thickness of the viable cell rim. This prediction compares well with the few experimental estimates of proliferating cell rims in spheroids (Freyer & Sutherland 1986a) and again emphasizes the fact that the viable rim size is only an upper bound on the size of the proliferating cell rim. As the autostimulation model includes the positive feedback mediated by cell–cell interactions, its successful applicability to data is compatible with the importance of cell–cell interactions in spheroid growth. This might be especially true because growth inhibition in spheroids has been experimentally demonstrated (Freyer & Sutherland 1986b, Freyer, Schor & Saponara 1988), yet purely inhibitory models do not describe overall spheroid growth adequately. Growth stimulating cell–cell interactions are a central tenet of the well documented autocrine hypothesis (cf. Bajzer & Vuk-Pavlović 1990, and references therein) and spheroids provide an excellent experimental system for systematic testing of the relative roles of stimulation and inhibition in regulation of tumour cell proliferation in three dimensions.

We also analysed the applicability of three structural models. The constant crust model was clearly inadequate and was not further analysed as were the models by Landry *et al.* (1982) and the simple spheroid model. The model by Landry *et al.* (1982) is based on rather detailed concepts in spheroid growth regulation, but for several data sets it yielded unacceptable values for the doubling time and the viable rim thickness. Moreover, for all data sets the χ^2 minimum was reached for $\eta = 0$; the reason for this peculiar behaviour is not clear. We created the simple spheroid model by modifying the constant crust model for the loss of cells from the spheroid. Application of the simple spheroid model resulted in a high correlation between calculated and experimental values for the viable rim thickness. Thus, it appears that the simple basic assumptions of this model are adequate and can provide a basis for further refinements of the model.

It is noteworthy that the simple spheroid model is structured similarly to the von Bertalanffy model. In the von Bertalanffy model, the growth increment is proportional to the spheroid surface ($V^{2/3}$), while in the simple spheroid model it is proportional to the volume of the proliferating cell rim. As this rim is rather thin and of constant thickness, its volume is roughly proportional to the surface. In both models, the loss of spheroid volume is proportional to the volume itself. Despite these similarities, the von Bertalanffy model proved inadequate for description of spheroid growth while the simple spheroid model was adequate. Thus, the critical difference in the applicability of these models must reside in the fact that the simple spheroid model encompasses exponential growth and/or that the volume of the proliferating cell rim is only approximately proportional to the spheroid surface.

Finally, we wish to emphasize the salient results of this study. First, our analysis shows how

one can meaningfully compare different mathematical models applicable to growth of tumour spheroids. In this work we: **1** classified the models into three groups (empirical, functional and structural); **2** introduced nesting of models wherever possible; **3** used rigourous statistical criteria for comparison of fits by the models, and **4** tested the predictions by the models against the available experimental data on cellular doubling times and thickness of proliferating cell rim. This approach made it possible to select the most preferable model in each group. We believe that this procedure is a methodological improvement in tumour growth modelling.

Secondly, we concluded that in the Gompertz model inherent is an important principle of biological growth. Namely, this model is definitely more adequate for description of spheroid growth than the von Bertalanffy model and the logistic model, although all three models have similar mathematical structure (exemplified through the generalized two-parameter model) and the same number of free parameters. Consequently, the three models should be similarly flexible in description of growth curves, yet only the Gompertz model was successful in description of the data.

Thirdly, the subtle preference of the autostimulation model among the functional models is compatible with a role of positive feedback mechanisms in cell–cell interactions, but also with the possibility that growth inhibition was not modelled adequately. However, the experimental evidence for growth stimulation by cell–cell interactions is overwhelming and further studies will evaluate more quantitatively the role of positive feedback mechanisms in regulation of spheroid growth.

ACKNOWLEDGEMENTS

We thank Drs J. S. Kovach and F. G. Prendergast for continuous friendly support, and K. Peters for help in preparation of figures. Supported by USPHS Grants CA45312 and CA51150 and by a grant by the Fraternal Order of Eagles.

REFERENCES

BAJZER Ž, VUK-PAVLOVIĆ S. (1990) Quantitative aspects of autocrine regulation in tumors. *CRC Crit. Rev. Oncogen.* **2**, 53.

BAJZER Ž, MARUŠIĆ M, VUK-PAVLOVIĆ S. (1994) Mathematical modelling of cellular interaction dynamics in multicellular tumor spheroids. In: Lakshmikantham V, ed. *Proceedings of the First World Congress of Nonlinear Analists*. Vol. 4 Berlin: Walter de Gruyter, in press.

VON BERTALANFFY L. (1941) Untersuchungen über die Gesetzlichkeit des Wachstums, VII, Stoffwechseltypen und Wachstumtypen. *Biol. Zentralbl.* **61**, 510.

VON BERTALANFFY L. (1957) Quantitative laws in metabolism and growth. *Q. Rev. Biol.* **32**, 217.

BISHOP YMM, FIENBERG SE, HOLLAND PW. (1975) *Discrete Multivariate Analysis: Theory and Practice*. Cambridge, MA: The MIT Press, 502.

BJERKVIG R ed. (1992) *Spheroid Culture in Cancer Research*. Boca Raton: CRC Press.

CASCIARI JJ, SOTIRCHOS SV, SUTHERLAND RM (1992) Mathematical modelling of microenvironment and growth in EMT6/Ro multicellular tumour spheroids. *Cell Prolif.* **25**, 1.

CONGER AD, ZISKIN MC (1983) Growth of mammalian multicellular tumor spheroids. *Cancer Res.* **43**, 556.

COOK RD, WEISBERG S. (1990) Linear and nonlinear regression. In: Berry DA, ed. *Statistical Methodology in the Pharmacological Sciences*, New York: Marcel Dekker, 163.

COX EB, WOODBURY MA, MYERS LE. (1980) A new model for tumor growth analysis based on a postulated inhibitory substance. *Comp. Biomed. Res.* **13**, 437.

DURBIN J, WATSON GS. (1950) Testing for serial correlation in least squares regression. I. *Biometrika*, **37**, 409.

DURBIN J, WATSON GS. (1951) Testing for serial correlation in least squares regression. II. *Biometrika*, **38**, 159.

FELLER W. (1940) On the logistic law of growth and its empirical verifications in biology. *Acta Biotheoretica*, **5**, 51.

FELLER W. (1971) *An Introduction to Probability Theory and its Applications*. New York: Wiley, 52.

FREYER JP. (1988) Role of necrosis in regulating the growth saturation of multicellular spheroids. *Cancer Res.* **48**, 2432.

FREYER JP, SCHOR PL. (1989) Regrowth kinetics of cells form different regions of multicellular spheroids of four cell lines. *J. Cell. Physiol.* **138**, 384.

FREYER JP, SCHOR PL, SAPONARA AG. (1988) Partial purification of a protein growth inhibitor from multicellular spheroids. *Biochem. Biophys. Res. Commun.* **152**, 463.

FREYER JP, SUTHERLAND RM. (1986a) Proliferative and clonogenic heterogeneity of cells form EMT6/Ro multicellular spheroids induced by the glucose and oxygen supply. *Cancer Res.* **46**, 3513.

FREYER JP, SUTHERLAND RM. (1986b) Regulation of growth saturation and development of necrosis by glucose and oxygen supply. *Cancer Res.* **46**, 3504.

GOMPERTZ B. (1825) On the nature of the function expressive of the law of human mortality. *Philos. Trans. R. Soc. Lond.* [*Biol.*], **36**, 513.

GYLLENBERG M, WEBB GF. (1989) Quiescence as an explanation of Gompertzian tumor growth. *Growth, Dev. Aging*, **53**, 25.

KREYSZIG E. (1970). *Introductory Mathematical Statistics.* New York: Wiley.

LANDRY J, FREYER JP, SUTHERLAND RM. (1982) A model for the growth of multicellular spheroids. *Cell Tissue Kinet.* **15**, 585.

MAGGELAKIS SA, ADAM JA. (1990) Mathematical model of prevascular growth of a spherical carcinoma. *Math. Comput. Modeling*, **13**, 23.

MARUŠIĆ M, BAJZER Ž. (1993) Generalized two-parameter equation of growth. *J. Math. Anal. Appl.* **179**, 446.

MARUŠIĆ M, BAJZER Ž, FREYER JP, VUK-PAVLOVIĆ S. (1991) Modeling autostimulation of growth in multicellular tumor spheroids. *Int. J. Biomed. Comput.* **29**, 149.

MICHELSON S, GLICKSMAN AS, LEITH JT. (1987) Growth in solid heterogeneous colon adenocarcinomas: comparison of simple logistical models. *Cell Tissue Kinet.* **20**, 343.

MORE JJ. (1977) The Levenberg-Marquardt algorithm, implementation and theory. In: Watson GA, ed. *Numerical Analysis*, New York: Springer.

PEARL R. (1924) *Studies in Human Biology.* Baltimore: Williams & Wilkins.

PIANTADOSI S. (1985) A model of growth with first-order birth and death rates. *Comp. Biomed. Res.* **18**, 220.

PIANTADOSI S. (1987) Generalizing growth functions assuming parameter heterogeneity. *Growth*, **51**, 50.

PRESS WH, FLANNERY BP, TEUKOLSKY SA, WETTERLING WT. (1986) *Numerical Recipes.* Cambridge: Cambridge University Press.

SAVAGEAU MA. (1979) Allometric morphogenesis of complex systems; a derivation of the basic equations from first principles. *Proc. Natl Acad. Sci.* **76**, 6023.

SCHWARTZ G. (1978) Estimating the dimension of a model. *Ann. Stat.* **6**, 461.

SHAMPINE LF, GORDON MK. (1975) *Computer Solution of Ordinary Differential Equations. The Initial Value Problem.* New York: Freeman.

STEEL GG. (1977). *Growth kinetics of tumors.* Oxford: Clarendon Press, 21.

SUTHERLAND RM. (1988) Cell and environment interactions in tumor microregions: the multicell spheroid model. *Science*, **240**, 177.

SWAN GW. (1990) Role of optimal control theory in cancer chemotherapy. *Math. Biosci.* **101**, 237.

TURNER ME Jr, BRADLEY EL Jr, KIRK KA, PRUITT KM. (1976) A theory of growth. *Math. Biosci.* **29**, 367.

VAIDYA VG, ALEXANDRO FJ Jr. (1982). Evaluation of some mathematical models for tumor growth. *Int. J. Biomed. Comput.* **13**, 19.

VERHULST PF. (1838) Notice sur la loi que la population suit dans son accroissement. *Corr. Math. Phys.* **10**, 113.

WHELDON TE. (1988) *Mathematical Models in Cancer Research.* Bristol: Adam Hilger.

WHELDON TE, KIRK J, GREY WM (1973) Mitotic autoregulation, growth control and neoplasia. *J. Theor. Biol.* **38**, 627.